

Microsystems for the Fabrication of Nano-Scale Structures

C.G. Courcimault, D.S. Kercher, M.G. Allen
School of Electrical and Computer Engineering
Georgia Institute of Technology, Atlanta, GA, 30332, USA

ABSTRACT

This paper describes fabrication and testing of microsystems which can be utilized for in-situ deposition control and direct patterning of structures with micron and submicron lateral and vertical dimensions. An electrostatically-driven microactuator acts as an addressable active shutter and shadow mask in a Physical Vapor Deposition system. The displacement of the actuator is controlled in the nano-scale range, without using electrical sensing circuitry, by means of 'stoppers' fabricated as integral parts of the structure. The deposition of metals through the real-time-actuated microsystem allowed control of the three dimensional shape of the deposited patterns as verified by AFM measurements.

INTRODUCTION

Microelectronics fabrication requirements have driven the continued development of tools for the realization of highly precise, reproducible, and scalable structures, typically in micron dimensions [1]. More recently, the fabrication of nano-scale structures has been under rapid development. Two main approaches have been investigated. The first approach is to improve the resolution of photolithographic techniques through wavelength reduction, e-beam lithography [2] and other similar techniques. The second approach is to chemically grow nano-scale structures from individual atoms and molecules [3], or to electrodeposit materials into nano-scale molds [4]. An alternative method of fabrication at this scale is to use micro-systems as tools for the fabrication of nano-systems. This approach was introduced by using batch fabricated AFM (Atomic Force Microscope) tips for etching of polymers [5] or metals [6].

In this paper we present microsystems for in-situ metal deposition control and direct patterning of structures with micron and submicron lateral dimensions, by means of actively-repositionable shadow masks integrally fabricated with the surface of a deposition substrate. Figure 1 shows the device concept. An electrostatically-driven microactuator acts as an addressable in-situ active shutter and shadow mask. Unlike previous static approaches [7], the shutter position is controllably varied during the deposition of films. The position of the mask can also be varied during the deposition of multiple materials. Since the mask can be surface micromachined onto the substrate, excellent alignment can be achieved, and transmission of the dynamic mask can occur with high fidelity.

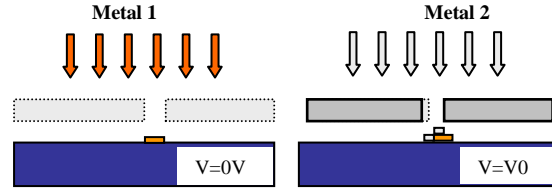


Figure 1 - Concept of the active shutter and shadow mask. a) A first deposition occurs when no voltage is applied. Deposited material reaches the substrate through the opening. b) A second deposition begins while the system is actuated. If the displacement of the opening is less than its width, overlap of the two metallic lines will take place.

DESIGN AND FABRICATION

Design

The design of the actuator focuses on the control of nano-scale displacements. When considering modes of actuation and displacement control, electrostatic clamping was chosen to ensure accurate control of the range of displacement.

Figure 2 shows a schematic of the microactuator. The microactuator is composed of three independent elements. The first element is a central annular shuttle consisting of a free-standing, electrically-grounded structure supported by four bending beams that allow in-plane shuttle displacement. Defined within the shuttle thickness is a set of rectangular openings allowing evaporated metal to reach the substrate. The pattern of the deposited film depends then on the displacement of the shuttle while depositions occur. The second element is composed of a series of fixed electrodes surrounding the moving shuttle, which are used for electrostatic drive of the actuator. The third element comprises fixed stoppers, held near electrical ground by a resistance meter. The stoppers are designed to be closer to the shuttle than the electrodes. When a voltage is applied to a single electrode, the shuttle clamps onto the nearest stopper. Electrostatic clamping ensures fixed displacement. In order to induce displacements of various amplitudes, the shuttle has been shaped as a circle. Its displacement is then defined by the position of the attractive electrode around the perimeter of the circle.

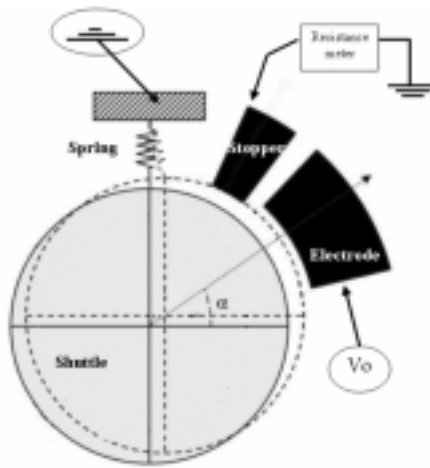


Figure 2 - Schematic of the microactuator design.

The displacement of the shuttle is given by:

$$x = g \cdot \cos \alpha \quad (1)$$

$$y = g \cdot \sin \alpha \quad (2)$$

where g is the gap between shuttle and stopper and α is the angle between electrode and the x-axis.

As mentioned above, the gaps between electrodes, stoppers and shuttle are defined by photolithography. The electrodes are designed to be 0.5 micron further away from the shuttle than the stoppers. Even though the gaps are on the order of a micron, the resulting displacement is controlled in the nano-scale range. The chart presented in Figure 3 shows how the shuttle displacement in the x-direction is controlled by the choice of the attracting electrode. The position of the shutter is indexed and mechanically defined; no electrical sensing circuitry is needed.

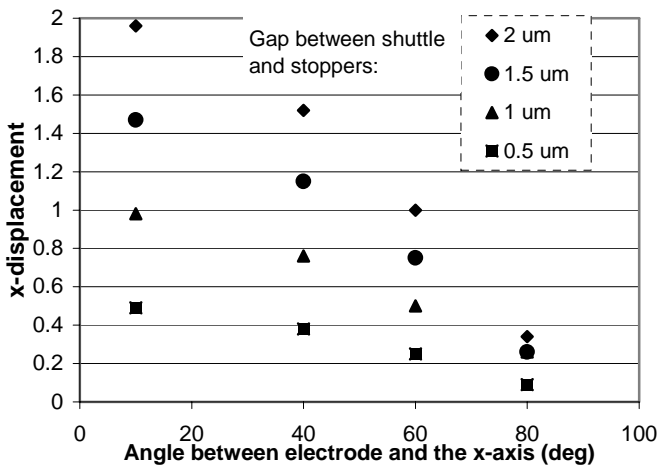


Figure 3 – Calculated indexed displacement (Eqs. 1 and 2) of the shuttle in the x-direction as a function of the gaps between stoppers and shuttle and the position of the attracting electrode.

In order to obtain the x- and y-displacements, the free-standing shuttle is mounted on crab-leg flexure beams. Because of fabrication constraints and the use of high resolution thin photo-resist, the total thickness of the device is limited to a few microns. The actuation voltage is kept relatively low by limiting the minimum arc length of each fixed electrode to 200 microns. In this manner the desired actuation can be achieved with relatively low applied voltages of tens of volts. Careful design of the flexure beams allows the shuttle to move and clamp on the stoppers.

Fabrication

The fabrication of the microactuator is designed to be low temperature, CMOS compatible, and allow a rapid turn-around due to the limited number of photolithography steps. Fabrication is based on the electrodeposition of nickel into photoresist molds (SPR 220-7, Shipley). The fabrication process is depicted Figure 4.

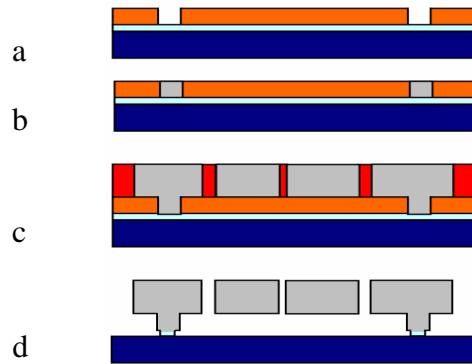


Figure 4 – Process flow.

First, a 300 nm silicon dioxide layer is deposited (PECVD) on a silicon wafer. A thin adhesion layer followed by a 2 um thick copper layer is then deposited using a sputtering system. This layer is a sacrificial layer that will eventually be removed to release the central shuttle. Photolithography and selective copper etching are performed to define openings for the anchors of the actuator. A second photolithography step defines a 6 to 8 micron thick electroplating mold (SPR 220-7, Shipley). Nickel is then electroplated into the mold (c). At this stage, the central circular electrode, the set of bending beams, the fixed electrodes and stoppers are complete. The photoresist and the sacrificial layer of copper are removed in order to release the suspended central shuttle. Finally, the silicon dioxide is wet etched in Buffered Oxide Etch (d) to expose the deposition substrate.

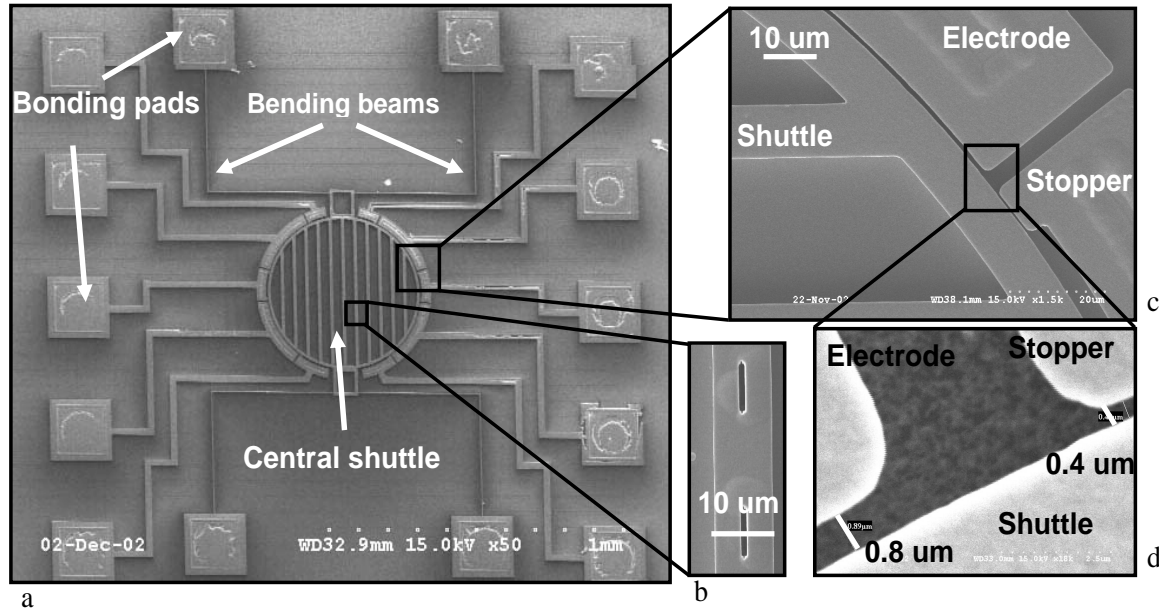


Figure 5 - a) Scanning Electron Micrograph of the overall microactuator. b) Electron micrograph of openings located in the center of the shuttle. c) SEM picture of the side of the shuttle. d) Close-up SEM picture showing the gaps between electrode, stopper, and shuttle.

FABRICATION RESULTS & TESTING

The results of fabrication are shown in Figure 5. An overall view of the device is shown on the Scanning Electron Micrograph of Figure 5a. The annular shuttle supported by a set of 4 bending beams is visible in the center. Each arm of the flexure is 250 microns long and 3 microns wide. Figure 5b is a close-up view of the central part of the shuttle. Openings are built in the thickness of the shuttle that allow the evaporated metal to reach the substrate. The openings are 1.1 microns wide and 10 microns long. The micrograph presented in Figure 5c shows a close-up view of the side of the shuttle. The gap between the stopper and shuttle is smaller than the gap between electrode and stopper. The SEM micrograph of Figure 5d shows that a 0.4 micron gap through a thickness of 6 microns (aspect-ratio: 1:15) has been achieved. Moreover, Figure 5d shows that even in this small size range, the electrode is 0.5 µm further away from the shuttle than the stoppers.

The microactuators have been tested under a probe station. DC actuation voltages for clamping range from 15 to 60 volts, depending on the design. The clamping is detected by looking at the resistance between the stoppers and the shuttle and detecting when this resistance falls from very high values.

EXPERIMENTAL SETUP AND RESULTS OF MULTI-LAYER NANOSCALE PATTERNING

Experimental setup

After testing, the microactuators were mounted and wire bonded into classic DIL packages. In order to protect the electrodes and pads from shorting while metal deposition occurs, the package is capped with a 50 micron thick Kapton film. A 200 x 200 micron square hole is etched by laser ablation into the Kapton film, and manually aligned to the center of the device. The package is connected to a solderless protoboard, and the board is then set into a filament evaporator. Electrical feedthroughs into the vacuum chamber allow remote operation of the microactuator. Figure 6 shows how the evaporated metal passes through the openings of the Kapton and the microsystem before reaching the substrate.

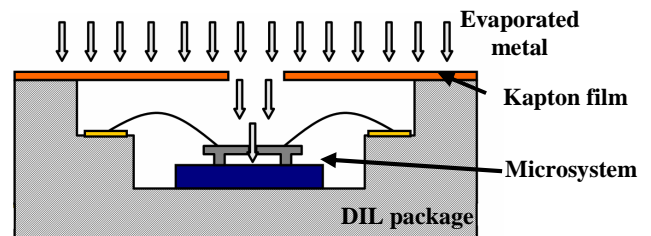


Figure 6 - Drawing of the cross-section of the encapsulated packaged microsystem during metal deposition.

Multi-layer nano-scale patterning

The microactuator, acting as a shadow-mask, allows the transmission of dynamic patterns while deposition occurs. Two experiments were conducted with two different devices.

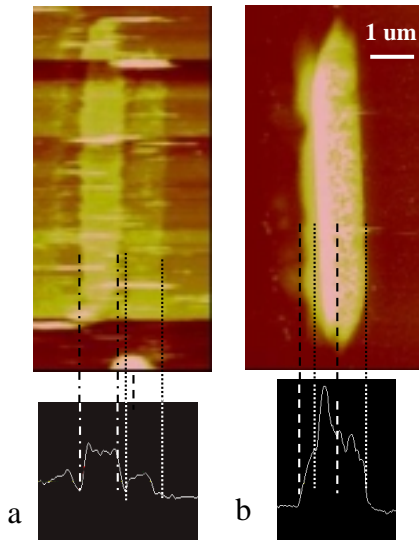


Figure 7 - AFM pictures and cross-section of the deposited metallic lines.

The device used in the first experiment presents a 2 μm gap between stoppers and the shuttle. The attracting electrode was fixed at a 40 degree angle from the x-axis. An actuation voltage of 60 volts allows clamping of the shuttle on the nearest stopper. The expected displacement of the shuttle in the x-direction is 1.5 micron. After setting the device in the PVD system, a 15nm thick layer of Cr was evaporated through the non-actuated device. The micro-system was then actuated, and without breaking vacuum, another layer of Cr (40 nm thick) was evaporated through the repositioned shuttle. When the deposition was completed, the sample was removed from the vacuum chamber. The microsystem was then manually removed and the deposited patterns were analyzed using an Atomic Force Microscope (AFM). Figure 7a shows the results. Two lines are deposited next to each other; each line is 1.1 μm wide and 10 μm long. The space between the two lines is 0.3 μm . The width of the opening being 1.1 μm , the displacement of the shuttle had to be 1.5 μm in order to form a 0.3 μm spacing between the two lines. This corresponds to the expected displacement of the actuator inside the PVD system.

A second experiment was conducted using another device. In this case the gap between stoppers and shuttle is 0.9 micron. The attracting electrode is fixed at a 40 degree angle from the x-axis. The clamping of the shuttle onto the nearest stopper required an applied voltage of 15 volts. The expected displacement of the shuttle in the x-direction is calculated to be 0.7 μm . Two different metals were deposited. First a 80 nm thick layer of Cr was

deposited through the non-actuated device, and then a 100 nm thick layer of Cu was evaporated through the repositioned shuttle. The results of the AFM study are shown in Figure 7b. Two 1.1 μm wide and 10 μm long lines are overlapping each other by 0.4 μm . In order to obtain this overlap, the opening had to move 0.7 μm over in the x-direction. The expected displacement of the shuttle inside the evaporator was 0.7 μm .

Accurate positioning of the shuttle, with no need for electrical sensing circuitry, has been demonstrated. By adjusting the displacement of the shuttle, the three-dimensional aspect of the multimaterial deposited patterns has been successfully controlled.

CONCLUSION

Electrostatically-driven microactuators, fabricated using conventional batch fabrication processes, have been used as tools for the fabrication of nano-scale structures. Using this approach, patterning of deposited films, varying spatially as well as compositionally, in the x, y, and z-dimensions were successfully demonstrated. Applications for this technology range from resonator tuning, to massive batch fabrication of multi-spectral emitter or detector elements, to nano-patterning of surface treatments for molecular and biological processes.

ACKNOWLEDGMENTS

This work was supported in part by the U.S. Defense Advanced Research Projects Agency under the NMAPS Program. Microfabrication was carried out in the Georgia Tech Microelectronics Research Center with the assistance of the staff.

REFERENCES

- [1] M.Madou, *Fundamentals of Microfabrication* (CRC Press, Boca Raton,FL),1997.
- [2] L.R. Harriott, "SCALPEL: projection electron beam lithography", Proc. of the Particle Accelerator Conference, 1999. pp 595 -599, vol.1.
- [3] E. C. Walter, B.J.Murray, F.Favier, M.R.Penner, "Noble and Coinage Metal Nanowires by Electrochemical Step Edge Decoration", J. Phys. Chem. B., 2002, 106(44); 11407-11411.
- [4] J. Schotter, T. Thurn-Albrecht, T. Russell, and M. Tuominen "Fabrication of nanoscale magnetic arrays by self-assembling polymers", submitted to Nature, 1999.
- [5] P.Vertiger "The Millipede – Nanotechnology Entering Data Storage" IEEE Transaction on nanotechnology. Vol 1, No 1, March 2002.
- [6] R. Schuster, V. Kirchner, X. H. Xia, A. M. Bittner, and G. Ertl: "Nanoscale Electrochemistry", Phys. Rev. Letters, vol.80, no.25, p.5599-602.
- [7] G.M. Kim, B.J. Kim, J. Brugger, "Photoplastic shadow-masks for rapid resistless multilayer micro patterning", Proc of Transducers 2001, Munich, pp 1632-1635.